Low cost and renewable sulfur-polymers by inverse vulcanisation

Supplementary Information

D. J. Parker[a], H. A. Jones[a], S. Petcher[a], L. Cervini[c], J. M. Griffin[c], R. Akhtar[b], and T. Hasell*[a]

[a] Department of Chemistry, University of Liverpool, Crown Street, Liverpool, L69 7ZD, UK email: T.Hasell@liverpool.ac.uk.
[b] Centre for Materials and Structures, School of Engineering, University of Liverpool, L69 3GH, UK.
[c] Department of Chemistry, Lancaster University, Lancaster LA1 4YB, U.K.

GPC analysis details and conditions:

Instrument: GPC analysis was performed on a Viscotek system comprising a GPCmax (degasser, eluent and sample delivery system), and a TDA302 detector array (column oven, light-scattering detectors, refractive index detector and viscometer). System eluent was analytical reagent grade chloroform (Fisher) and used as received. System columns were 2x T6000M plus Tguard (Malvern). OmniSEC v5.1 was used for instrument control, sample analysis and reporting.
Sample preparation: Materials were first separated into soluble/insoluble fractions by stirring for 3 hours in chloroform, before filtration through 0.45 μm PTFE, and evaporation to dryness. Aliquots of the GPC system eluent were then added to the soluble fraction to make the samples up to known concentration (nominally 5 mg/ml). The samples were left to dissolve at room temperature with gentle agitation for minimum of 2 hours. Samples were visually inspected to ensure they were completely dissolved. Samples were filtered into analysis vials through a 0.45 μm PTFE filter using a glass syringe.
Analysis conditions: System flow rate was 1 ml/min. Samples were stored and injected at room temperature. Columns and detectors were stabilised at 40 °C. Injection volume was 100 μL. Samples were analysed in duplicate.
Calibration method: Instrument calibration was performed using a PolyCAL PS105K narrow polystyrene reference sample (TDS-PS-N, Malvern). A 12-point polystyrene conventional calibration curve was generated using EasiVial PS-H standards (PL2010-0201, Agilent).
Result reporting: GPC baselines and limits were manually chosen to represent the >95 % of the sample peak. Default calculation parameters were used, and no addition smoothing or prediction algorithms were applied.

Solid-State NMR Experimental Details:

^{1}H and ^{13}C magic-angle spinning (MAS) NMR spectra were performed on a Bruker Avance III operating at a ^{1}H Larmor frequency of 700 MHz, using a Bruker 4mm HX probe. Chemical shifts were referenced using the CH_3 resonance of solid alanine at 1.1 ppm (^{1}H) and 20.5 ppm (^{13}C).

The ^{13}C NMR spectrum was recorded at a MAS rate of 5 ms using cross polarization (CP) to transfer magnetization from ^{1}H with a contact time of 5 ms. ^{1}H heteronuclear decoupling using

two-pulse phase modulation and a radiofrequency field strength of 100 kHz was applied during acquisition.

The ^{1}H MAS NMR spectrum was recorded at a MAS frequency of 9881 Hz with DUMBO homonuclear decoupling[1] applied to achieve high resolution. An empirically-determined scaling factor of 0.44 was applied to the ^{1}H chemical shifts.

The ^{1}H-^{13}C heteronuclear correlation spectrum was recorded at a MAS frequency of 11363 Hz with a CP contact time of 50 μs to favour directly-bonded correlations. DUMBO homonuclear decoupling was applied during t_1 and the 1H chemical shift axis was scaled to match the one-dimensional spectrum. ^{1}H heteronuclear decoupling using two-pulse phase modulation and a radiofrequency field strength of 100 kHz was applied during acquisition of the ^{13}C signal in the direct dimension.

DFT calculations on polymer fragments:

Computational calculations on the structural fragments were performed using Gaussian 09. Structures were generated using the GaussView package and fully optimized at the B3LYP level of theory using the 6-31G(d) basis set, before NMR parameters were calculated under the same conditions. For each polymer fragment shown in Scheme 2, cross-linking bonds were terminated with S-H groups prior to the calculations. A chemical shielding reference of 189.7 ppm was used, determined from a separate calculation on and optimized tetramethylsilane molecule.

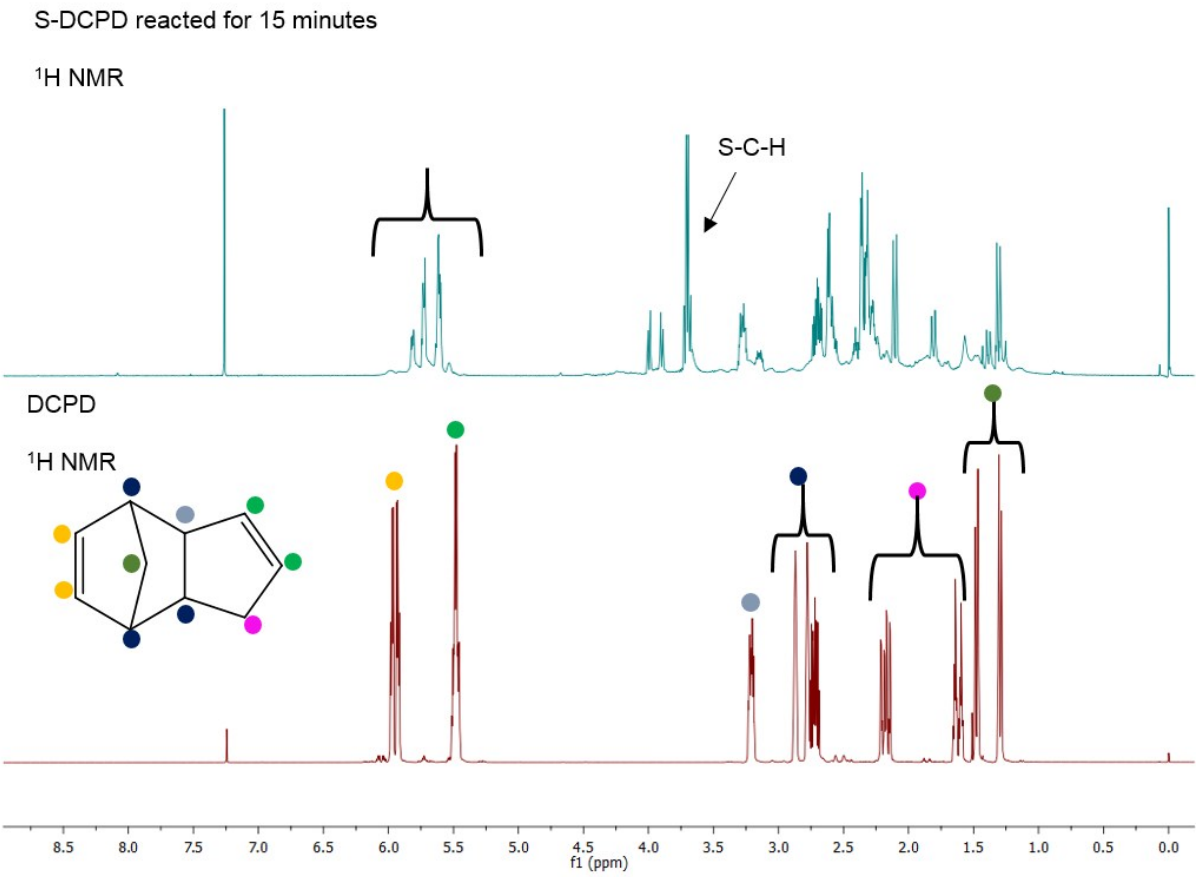

Figure S1: ^{1}H NMR spectra, in $CDCl_3$, for DCPD monomer and S-DCPD reaction products of a 15 minute reaction at 160 °C. There is a distinct shift in the peaks for the protons adjacent to the DCPD double bonds δ ~ 5.0-6.0 ppm suggesting some reaction of sulfur across the DCPD double bonds. However, it appears that one of the original peaks may have mostly disappeared whereas the other has shifted which signifies the reaction of sulfur across predominantly only one of the DCPD double bonds which supports the assumption that at shorter reaction times the S-DCPD polymers are less crosslinked explaining their solubility in chloroform. The formation of peaks at δ ~ 3.5 - 4.0 ppm is consistent with S-C-H protons, confirming the reaction between DCPD and sulfur.

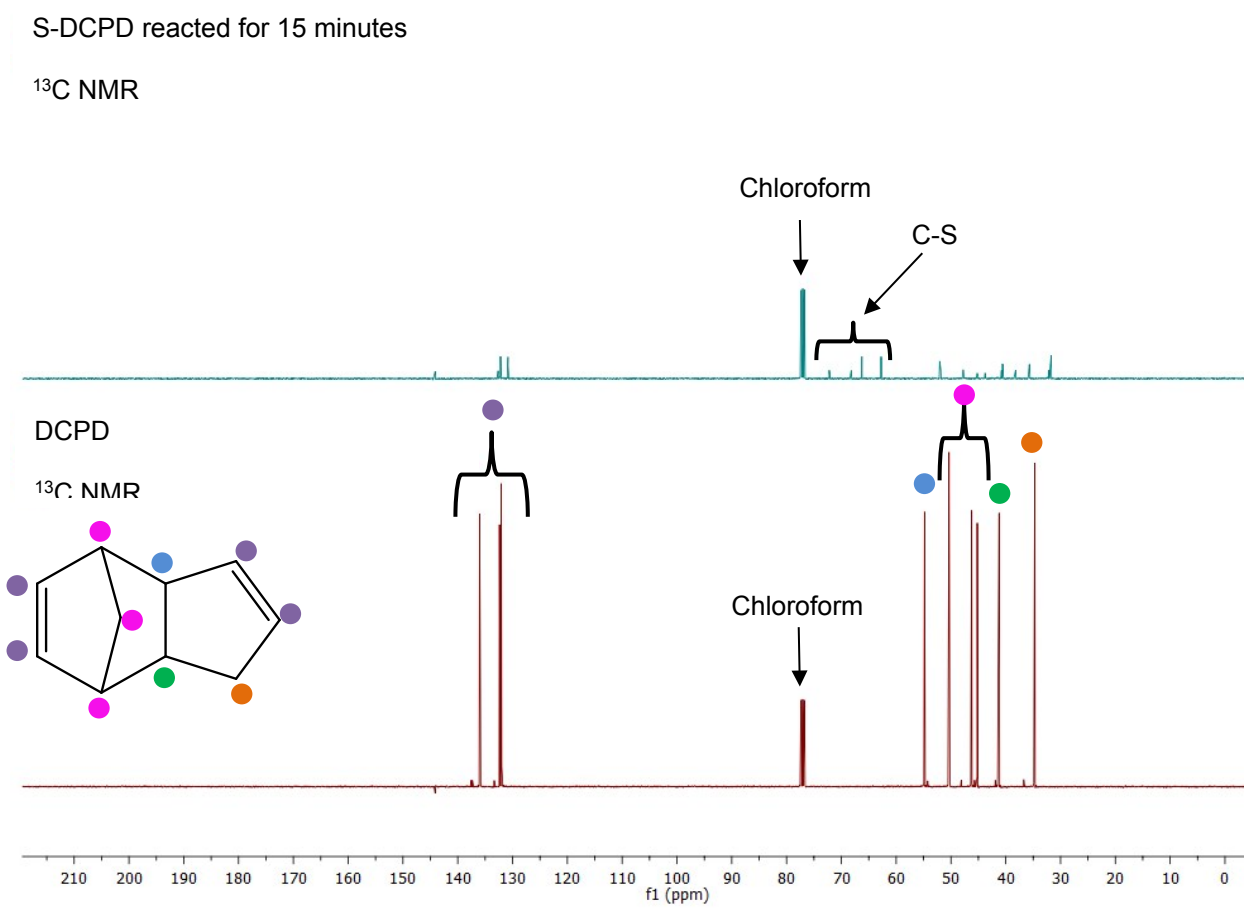

Figure S2: ^{13}C spectra for DCPD monomer and S-DCPD reaction products after 15 minutes at 160 °C, showing the formation of C-S bonds in the S-DCPD spectrum around 60 - 70 ppm. Similarly to the ^{1}H NMR spectrum, the DCPD double bond peaks have shifted but not disappeared altogether implying partial reaction.

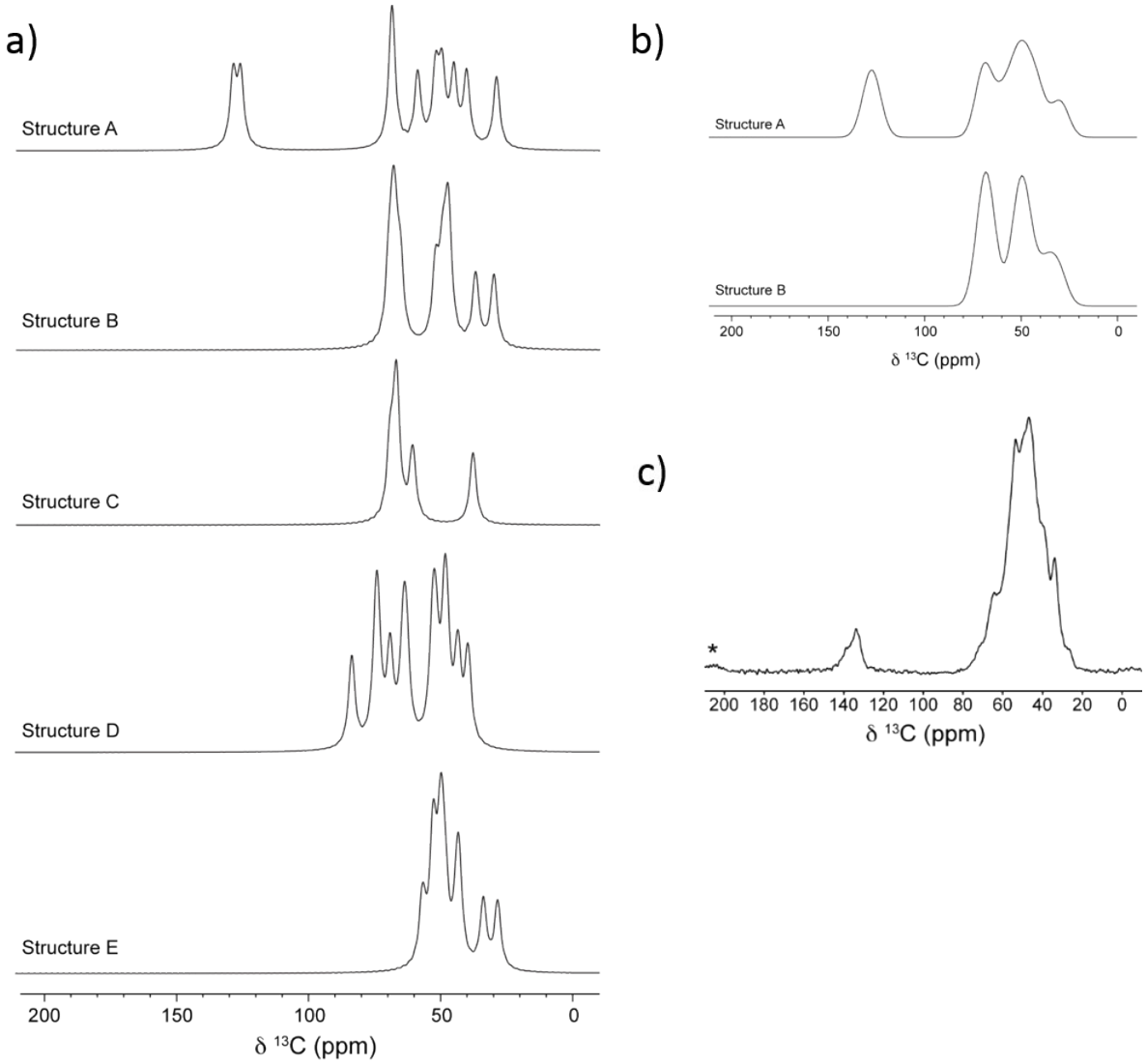

Figure S3: a) Simulated 13C NMR spectra based on optimized models of the polymer fragments shown in scheme 2 of the main paper. b) Simulated spectra for structures A and B with 200 Hz Gaussian line broadening to allow clearer comparison to the experimental spectra, shown in c).

For structures D and E, resonances corresponding to methyl groups (at around ~20 ppm) that where added to terminate the polymer fragment for the DFT calculations have been removed for clarity, since these would not be expected to be present in the materials. In the actual samples, these would be expected to give rise to R_2CH_2 groups instead, and will appear further downfield. The highest upfield signal for simulated structures A and B corresponds to the bridging CH_2 of the norborane substituent. This signal is absent for the structures C, D, and E which have lost the norborane substituent through cracking or ring opening polymerization. The presence of this peak in the experimental sample therefore suggests a high component of structures A and B.

Table S1. Solubility of S-polymers in various solvents.

	Crosslinker						
Solvent	*	DIB	DCPD	Limonene	Myrcene	Farnesene	Farnesol
	Acetone	1.6	IS	trace	IS	trace	trace
	Acetonitrile	10.9	IS	trace	IS	IS	IS
	Chloroform	9.7	IS	>17.2	9.7	20.8	25.7
	Hexane	IS	IS	trace	trace	trace	trace
	Methanol	IS	IS	trace	IS	IS	IS
	THF	10.5	IS	>12.4	11.7	16.8	25.1
	Toluene	13.6	IS	>16.1	12	19.6	13
	Water	IS	IS	IS	IS	IS	IS

* Determined by placing >100 mg of solid in 10 mL solvent and stirring overnight. Solubilities given in mg/mL, IS = insoluble, trace = colour visible in solution but <1 mg/mL residue.

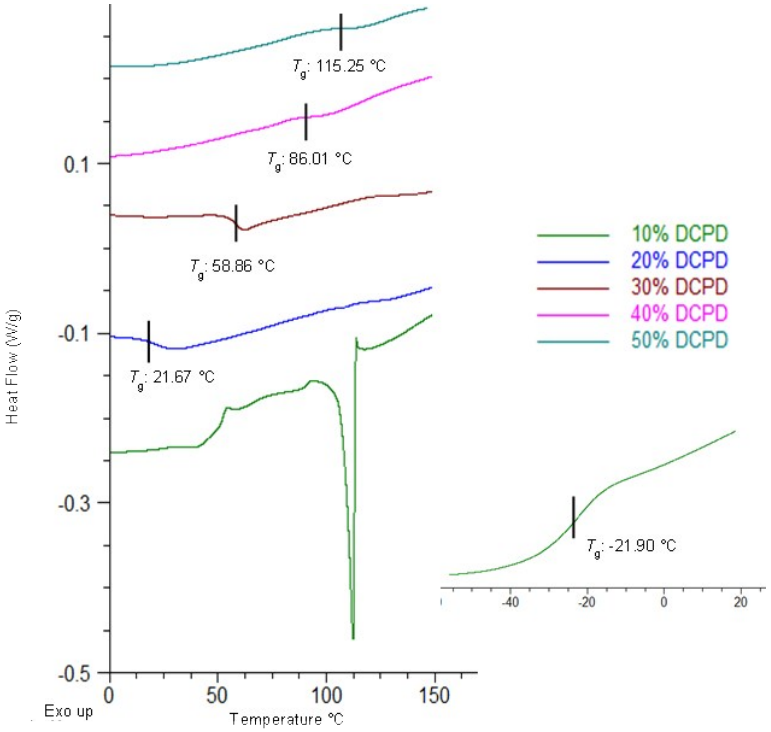

Figure S4. DSC traces of poly(S-DCPD) with varying S_8 content, inset on the right shows the lower temperature section of the 10 wt% DCPD sample in order to distinguish the T_g more clearly. The monoclinic S_8 crystalline melting transition T_m is clearly visible for the 10 wt % DCPD sample, but not present in the other materials.

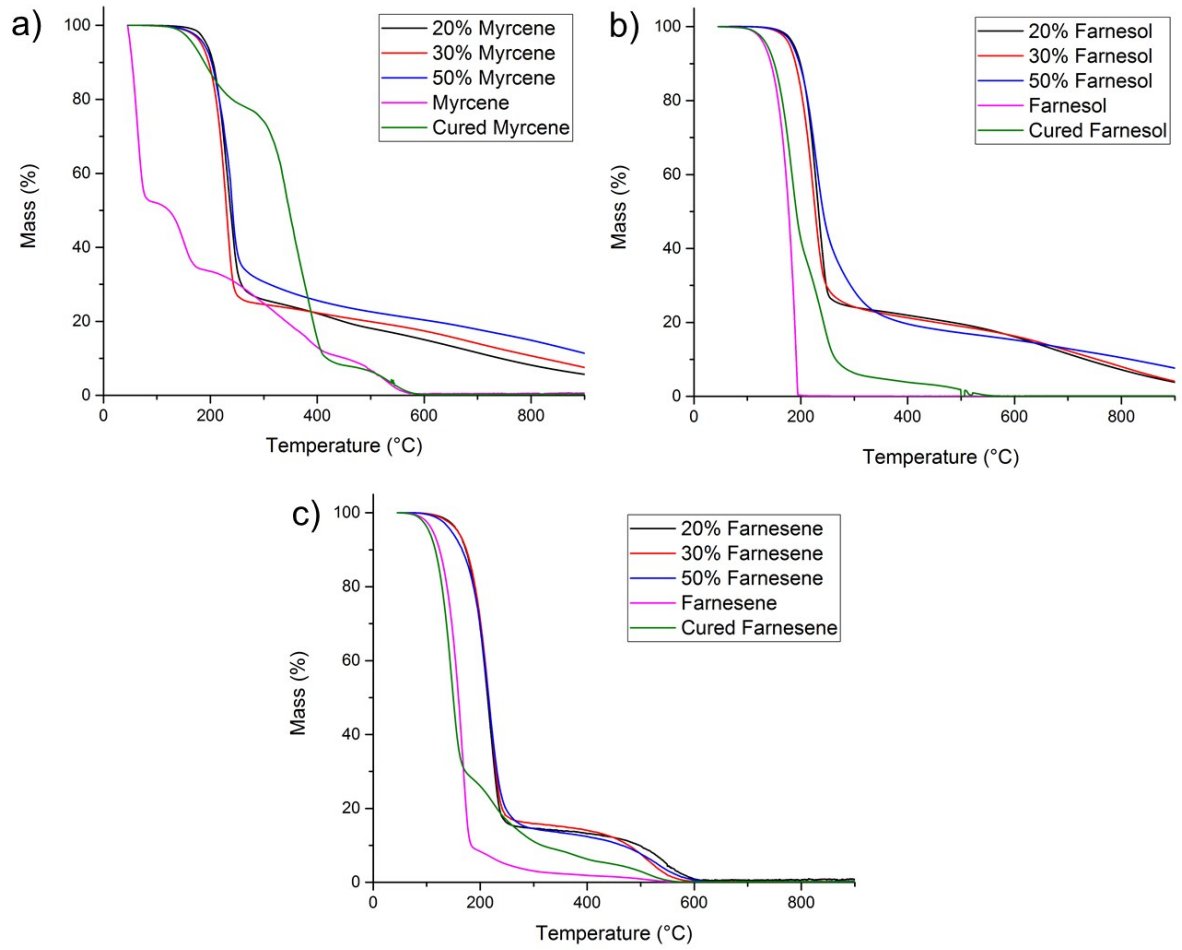

Figure S5. Thermogravimetric analysis of sulfur-renewable co-polymers and monomers: a) myrcene, b) farnesol, and c) farnesene. All run under nitrogen, at 10 °C/min.

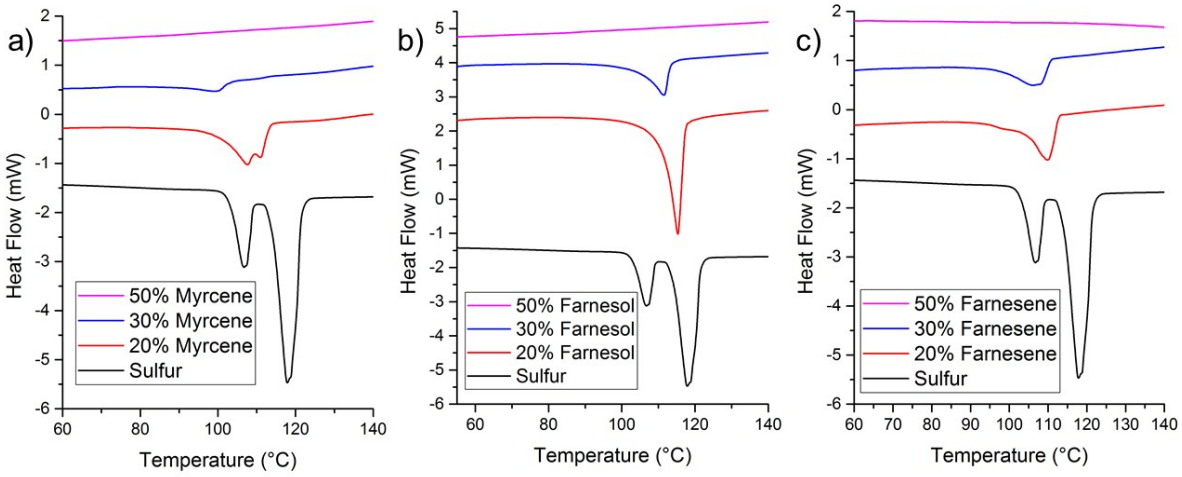

Figure S6. DSC traces of sulfur-renewable copolymers with varying S_8 content, showing the S_8 crystalline melting transition T_m region for: a) S-myrcene, b) S-farnesol, and c) S-farnesene. All polymers show no S_8 separation at 50 wt% crosslinker.

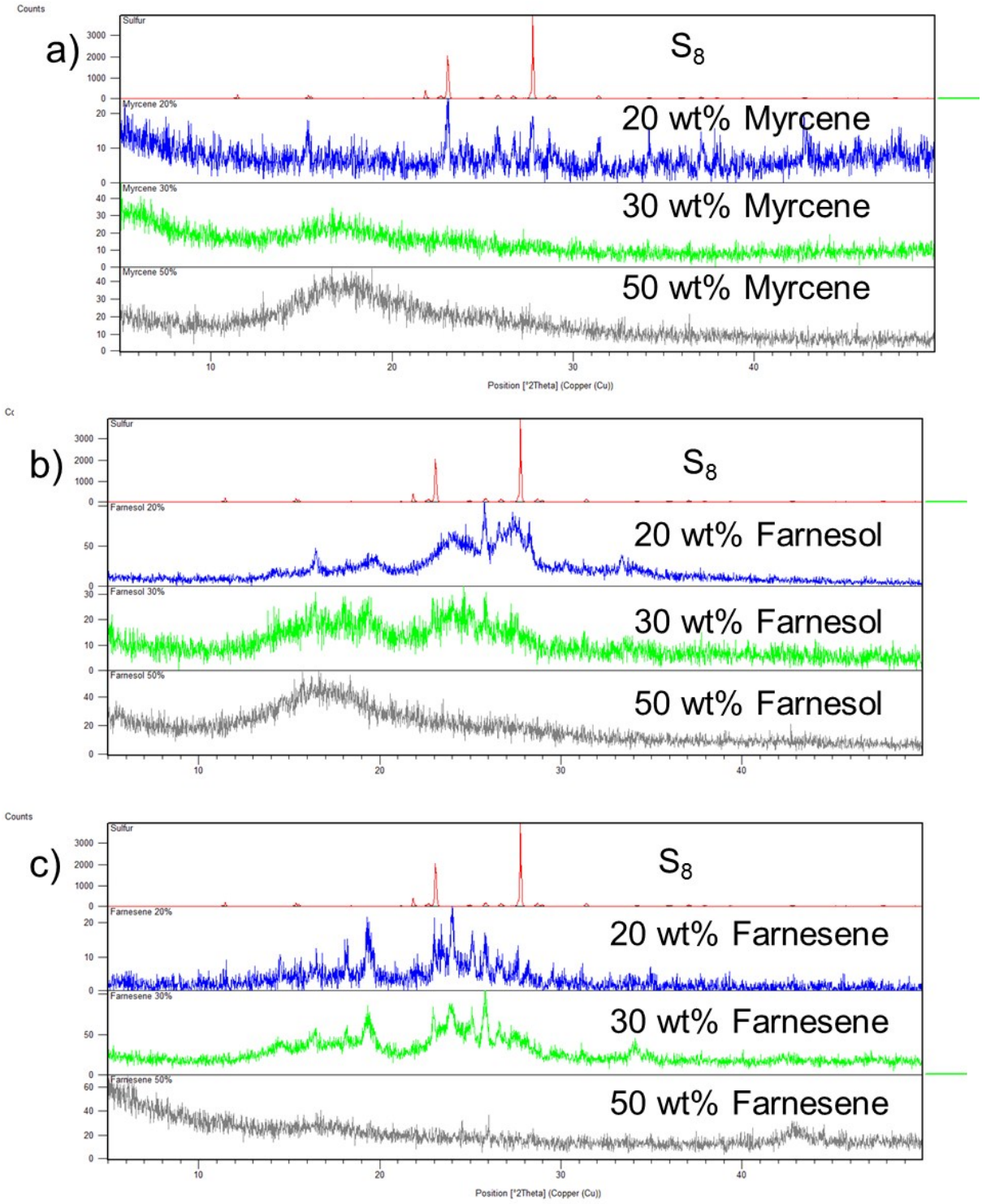

Figure S7. PXRD patterns of sulfur-renewable copolymers with varying S_8 content for: a) S-myrcene, b) S-farnesol, and c) S-farnesene. At 20 wt% crosslinker all 3 polymers show traces of crystalline sulfur. At 30 wt% crosslinker S-farnesene shows most crystallinity, with only slight signal from S-farnesol, and only amorphous material for S-myrcene. All polymers show no crystallinity (and therefore S_8 separation) at 50 wt% crosslinker.

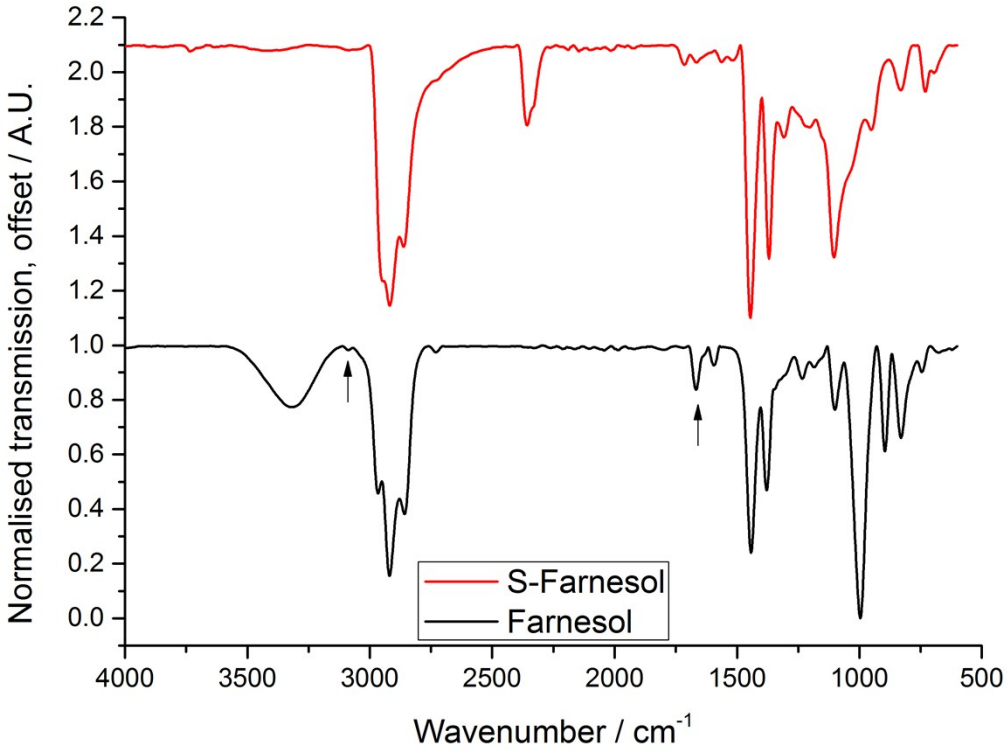

Figure S8. FT-IR spectra of 50 wt.% Sulfur, 50 wt.% farnesol co-polymer (top), compared to unreacted farnesol (bottom). Loss of the peaks associated with =C-H and C=C stretching vibrations at ~3090 and 1665 cm^{-1}, respectively, can be noted. Additionally, there is a loss of the broad alcohol O-H stretch at 3320 cm^{-1} and an associated shift of the peak at 995 cm^{-1} to 1100 cm^{-1} corresponding to the transformation of the alcohol group to an ether.

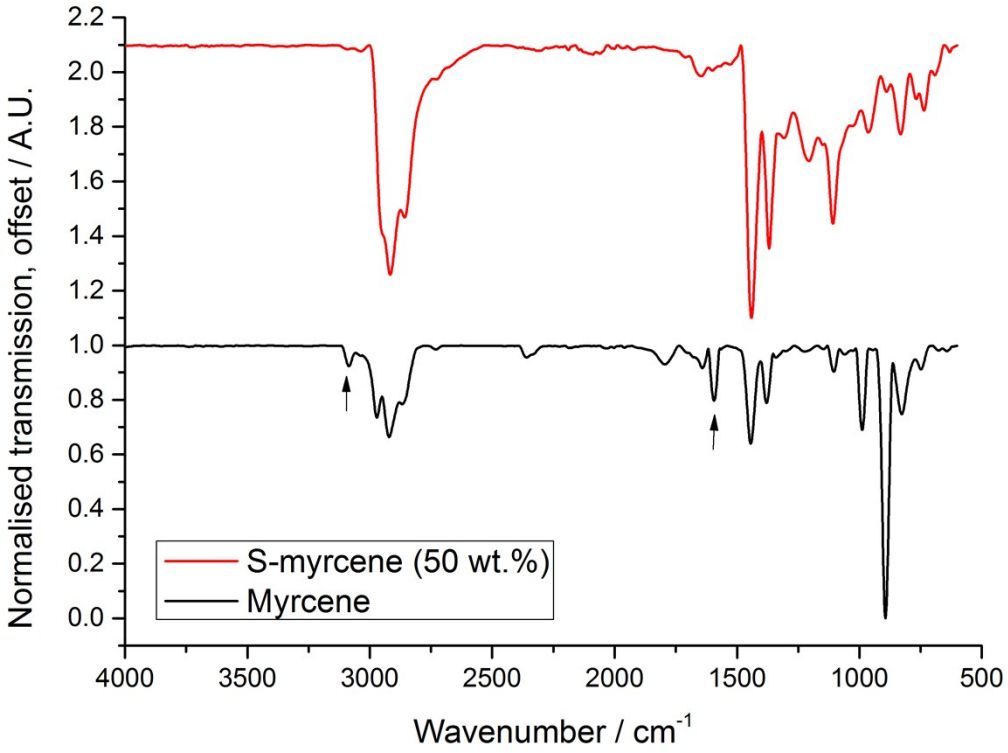

Figure S9. FT-IR spectra of 50 wt.% Sulfur, 50 wt.% myrcene co-polymer (top), compared to unreacted myrcene (bottom). Loss of the peaks associated with =C-H and C=C stretching vibrations at ~3090 and 1590 cm^{-1}, respectively, can be noted.

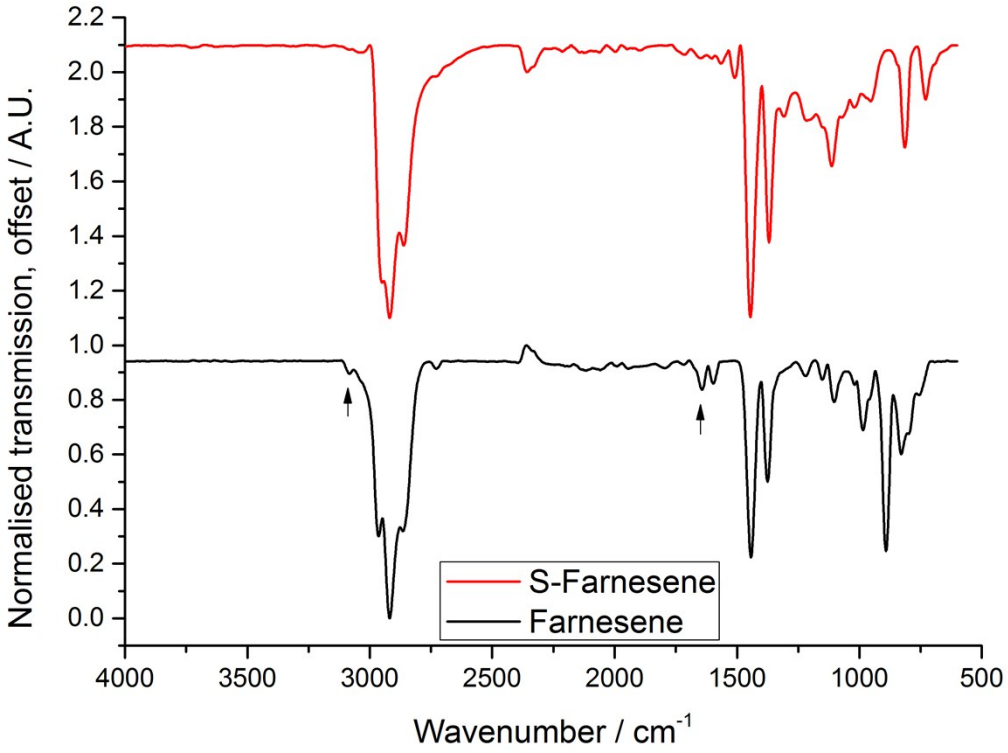

Figure S10. FT-IR spectra of 50 wt.% Sulfur, 50 wt.% myrcene co-polymer (top), compared to unreacted myrcene (bottom). Loss of the peaks associated with =C-H and C=C stretching vibrations at ~3080 and 1640 cm^{-1}, respectively, can be noted.

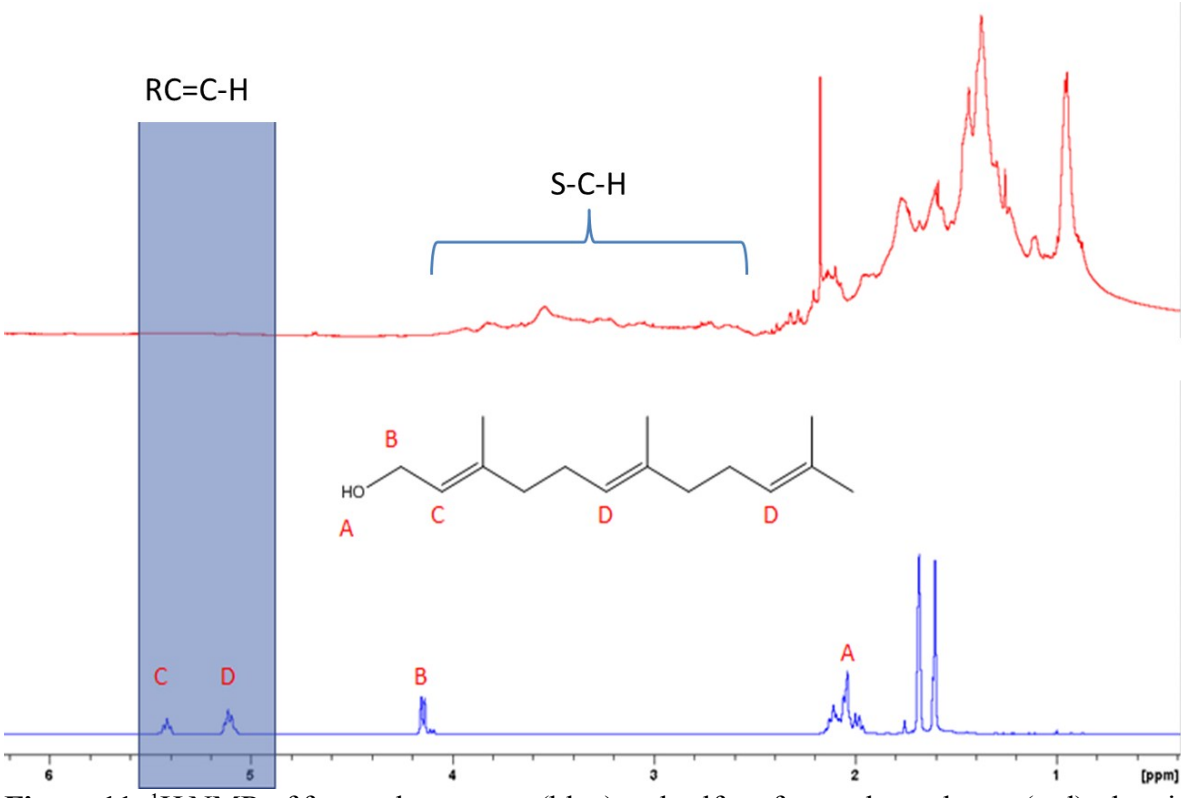

Figure 11: [1]H NMR of farnesol monomer (blue) and sulfur - farnesol copolymer (red), showing loss of double bonds and formation of C-S bonds.

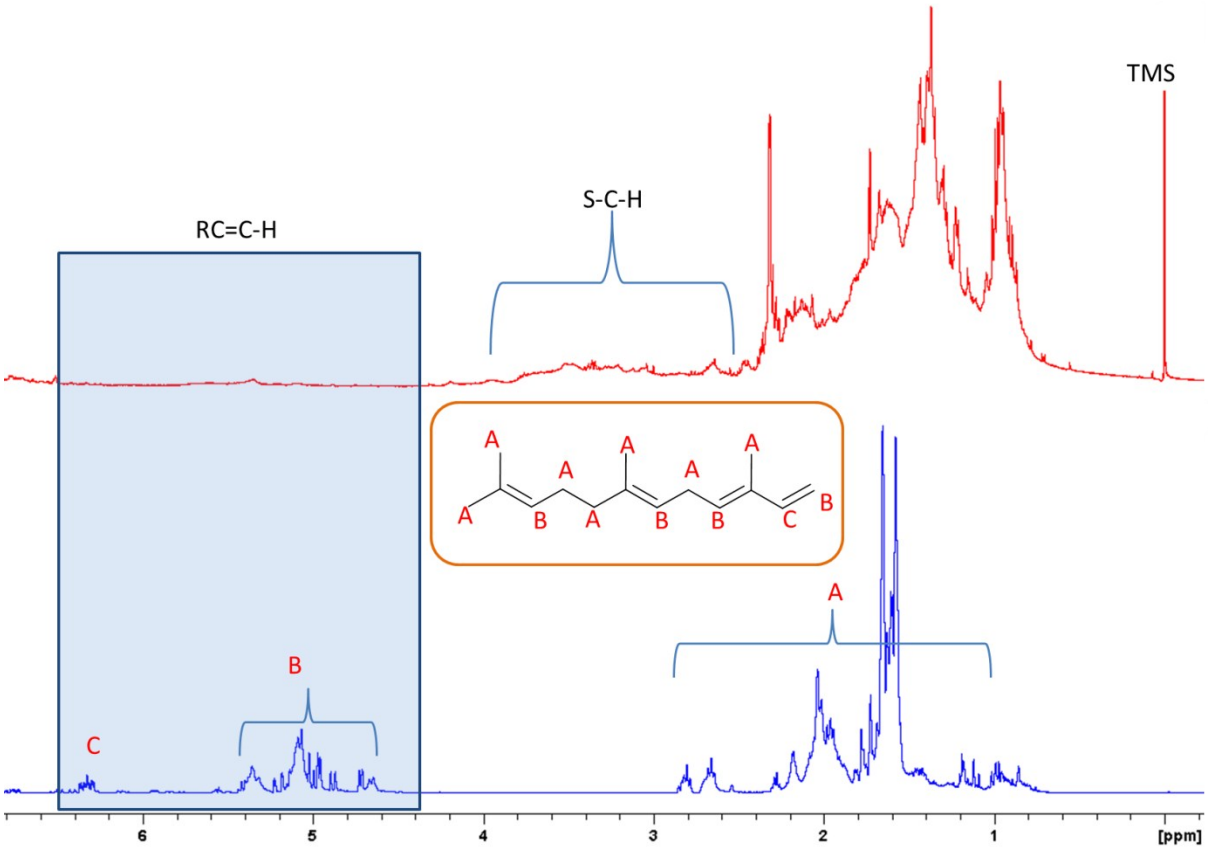

Figure 12: [1]H NMR of farnesene monomer (blue) and sulfur - farnesene copolymer (red), showing loss of double bonds and formation of C-S bonds.

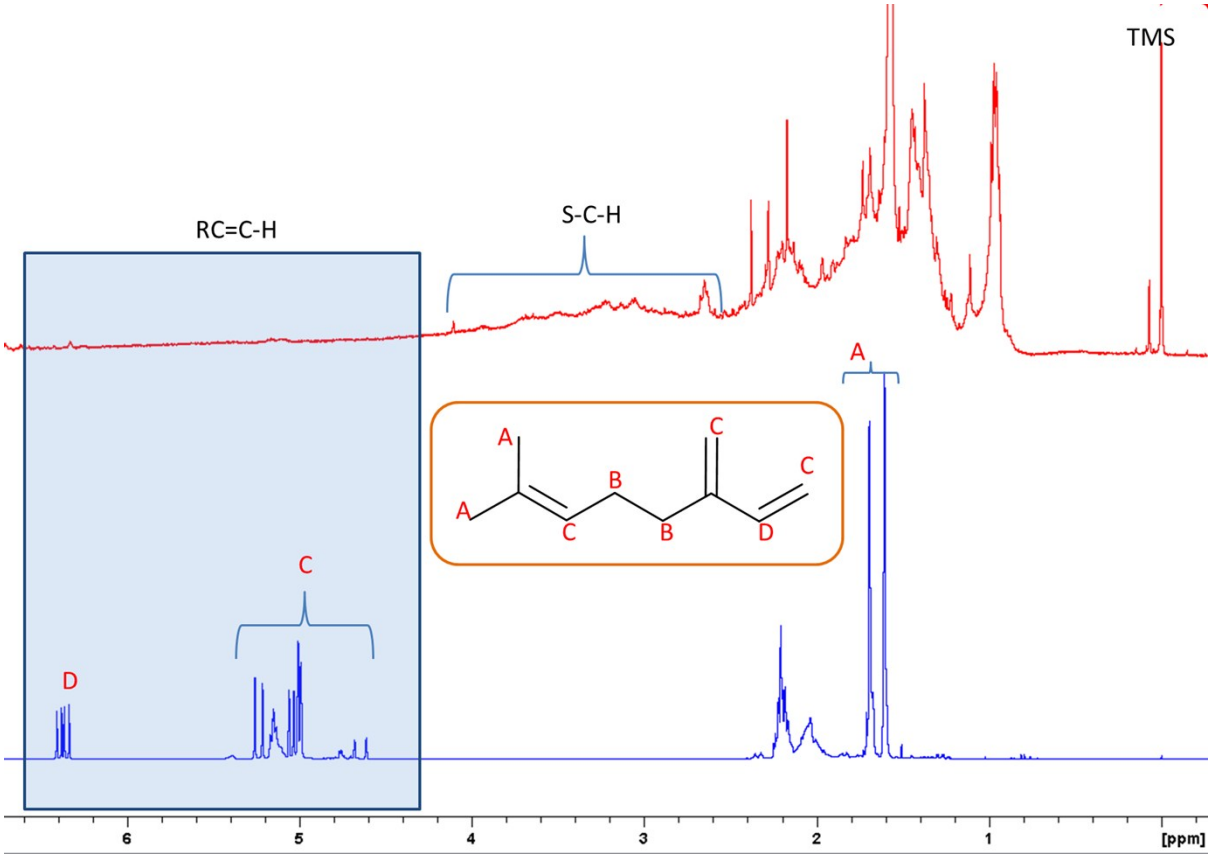

Figure 13: ^{1}H NMR of myrsene monomer (blue) and sulfur - myrcene copolymer (red), showing loss of double bonds and formation of C-S bonds.

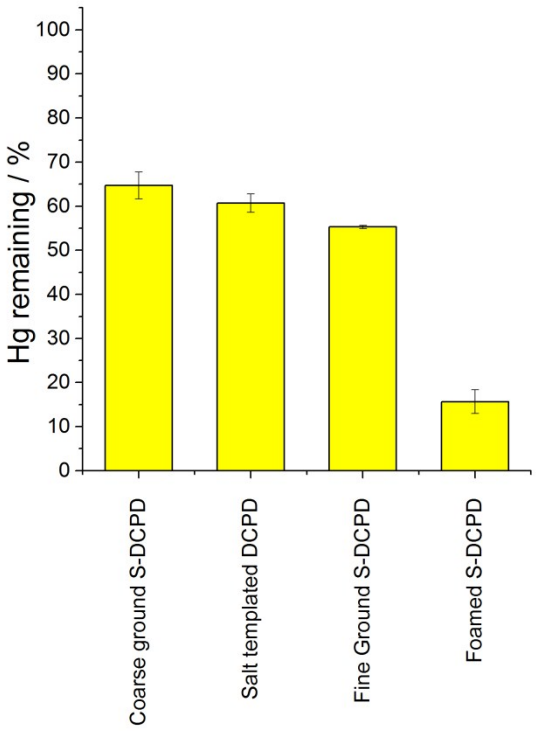

Figure S14. The percentage mercury remaining in solution after 3 hours exposure to each of the materials listed. Values are given as a mean of three repeats with standard deviation shown as error bars. Given the apparently higher level of connected porosity from the SEM imaging, it is unclear why more mercury is not taken up by the salt templated samples in comparison to the foamed samples. This could be a factor of wettability – with the aqueous solution not penetrating fully into the structure. Alternatively, there may be some action of the supercritical process to remove trace amounts of un-secured sulfur that could be taken into the solution phase and stabilise the Hg. These will be investigated fully in ongoing work.

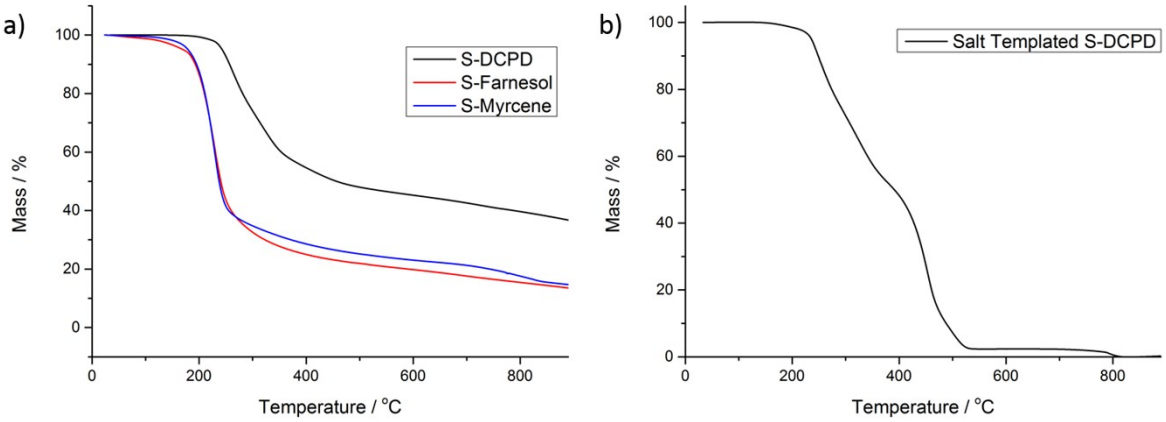

Figure S15. Thermogravimetric analysis of sulfur co-polymers: a) after CO_2 foaming, run under nitrogen, at 10 °C/min, and b) after salt templating, run under air, at 10 °C/min. There

is no significant change in the polymers after CO_2 foaming. After salt templating ~2 wt.% salt can be seen to be still trapped inside the polymer after washing (this remains after the rest of the polymer has fully decomposed by 600 °C, but is lost at ~800 °C as it melts).

1. B. Elena, G. de Paëpe and L. Emsley, *Chem. Phys. Lett.*, 2004, **398**, 532-538.